



Published in final edited form as:

J Bone Miner Res. 2015 April ; 30(4): 681–689. doi:10.1002/jbmr.2396.

Sclerostin Inhibition Prevents Spinal Cord Injury-Induced Cancellous Bone Loss

Luke A Beggs^{1,2}, Fan Ye^{1,2}, Payal Ghosh^{1,2}, Darren T Beck^{3,4}, Christine F Conover¹, Alexander Balazs¹, Julie R Miller¹, Ean G Phillips¹, Nigel Zheng⁵, Alyssa A Williams⁶, Jignacio Aguirre⁶, Thomas J Wronski⁶, Prodip K Bose^{1,6,7}, Stephen E Borst^{1,3}, Joshua F Yarrow^{1,2}

¹Research Service, Department of Veterans Affairs Medical Center, North Florida/South Georgia Veterans Health System, Gainesville, FL, USA

²Department of Applied Physiology and Kinesiology, University of Florida, Gainesville, FL, USA

³Geriatrics Research, Education, and Clinical Center (GRECC), Department of Veterans Affairs Medical Center, North Florida/South Georgia Veterans Health System, Gainesville, FL, USA

⁴Department of Kinesiology, University of Rhode Island, Kingston, RI, USA

⁵Department of Mechanical Engineering and Engineering Science, University of North Carolina at Charlotte, Charlotte NC, USA

⁶Department of Physiological Sciences, University of Florida, Gainesville, FL, USA

⁷Department of Neurology, University of Florida, Gainesville, FL, USA

Abstract

Spinal cord injury (SCI) results in rapid and extensive sublesional bone loss. Sclerostin, an osteocyte-derived glycoprotein that negatively regulates intraskeletal Wnt signaling, is elevated after SCI and may represent a mechanism underlying this excessive bone loss. However, it remains unknown whether pharmacologic sclerostin inhibition ameliorates bone loss subsequent to SCI. Our primary purposes were to determine whether a sclerostin antibody (Scl-Ab) prevents hindlimb cancellous bone loss in a rodent SCI model and to compare the effects of a Scl-Ab to that of testosterone-enanthate (TE), an agent that we have previously shown prevents SCI-induced bone loss. Fifty-five ($n = 11$ – 19 /group) skeletally mature male Sprague-Dawley rats were randomized to receive: (A) SHAM surgery (T8 laminectomy), (B) moderate-severe (250 kilodyne) SCI, (C) 250 kilodyne SCI + TE (7.0 mg/wk, im), or (D) 250 kilodyne SCI + Scl-Ab (25 mg/kg, twice weekly, sc) for 3 weeks. Twenty-one days post-injury, SCI animals exhibited reduced hindlimb

Address correspondence to: Joshua F Yarrow, PhD, North Florida/South Georgia Veterans Health System, 1601 SW Archer Road, Research-151, Gainesville, FL 32608-1197, USA. jfyarrow@ufl.edu.

Authors' roles: Study design: LAB, TJW, PKB, SEB, and JFY. Study conduct: LAB, FY, PG, DTB, CFC, AB, JRM, and EGP. Data collection: LAB, PG, DTB, CFC, AB, JRM, EGP, NZ, AAW, JIA, and TJW. Data analysis: LAB, FY, NZ, AAW, TJW, PKB, SEB, and JFY. Data interpretation: LAB, NZ, JIA, TJW, PKB, SEB, and JFY. Drafting manuscript: LAB and JFY. Revising manuscript: LAB, FY, PG, DTB, CFC, AB, JRM, EGP, NZ, AAW, JIA, TJW, PKB, SEB, and JFY. Approving final version of manuscript: LAB, TJW, PKB, SEB, and JFY. LAB and JFY take responsibility for the integrity of the data analysis.

Disclosures

All authors state that they have no conflicts of interest.

Additional Supporting Information may be found in the online version of this article.

cancellous bone volume at the proximal tibia (via μ CT and histomorphometry) and distal femur (via μ CT), characterized by reduced trabecular number and thickness. SCI also reduced trabecular connectivity and platelike trabecular structures, indicating diminished structural integrity of the remaining cancellous network, and produced deficits in cortical bone (femoral diaphysis) strength. Scl-Ab and TE both prevented SCI-induced cancellous bone loss, albeit via differing mechanisms. Specifically, Scl-Ab increased osteoblast surface and bone formation, indicating direct bone anabolic effects, whereas TE reduced osteoclast surface with minimal effect on bone formation, indicating antiresorptive effects. The deleterious microarchitectural alterations in the trabecular network were also prevented in SCI + Scl-Ab and SCI + TE animals, whereas only Scl-Ab completely prevented the reduction in cortical bone strength. Our findings provide the first evidence indicating that sclerostin inhibition represents a viable treatment to prevent SCI-induced cancellous and cortical bone deficits and provides preliminary rationale for future clinical trials focused on evaluating whether Scl-Ab prevents osteoporosis in the SCI population.

Keywords

PRECLINICAL STUDIES; OSTEOPOROSIS; ANABOLIC; HISTOMORPHOMETRY; MICROCOMPUTED TOMOGRAPHY

Introduction

Spinal cord injury (SCI) results in a host of deleterious musculoskeletal consequences, of which severe bone loss and high fracture risk occur nearly universally in skeletal tissue innervated below the level of the spinal lesion (ie, sublesionally).⁽¹⁾ Clinically, SCI-induced bone loss results from an uncoupling of bone turnover that is characterized by elevated bone resorption and normal to slightly reduced bone formation,⁽¹⁾ which produces 2% to 4% cancellous bone loss *per month* and results in a 40% to 70% lower cancellous bone mineral density (BMD) within several years of injury,⁽²⁾ with more gradual cortical bone loss that persists for more than a decade.⁽³⁾ As a result, individuals with functionally complete SCI have a 20- to 100-fold greater fracture risk than age-matched ambulatory individuals,⁽⁴⁾ with nearly 50% of those with SCI experiencing one or more low-trauma fractures at some point after injury.⁽⁵⁾ Interestingly, the distal femur and proximal tibia appear most susceptible to bone loss after SCI,⁽²⁾ accounting for >65% of all fractures requiring hospitalization in this population.⁽⁶⁾

Although the molecular mechanisms underlying SCI-induced bone loss have not been adequately elucidated,⁽⁷⁾ diminished Wnt signaling⁽⁸⁾ appears to be involved in osteoblast dysfunction after SCI.^(9,10) Sclerostin, an osteocyte-derived Wnt-signaling pathway antagonist and negative regulator of bone formation,⁽⁷⁾ is elevated in men after SCI.^(11,12) Circulating sclerostin appears highest in men in the first 5 years after SCI,⁽¹²⁾ coinciding with the time during which the most rapid bone loss occurs clinically after injury, and is lowest in men with chronic SCI-induced osteoporosis,^(11,12) likely because of low osteocyte expression in those with severe bone loss. Similarly, rodents exhibit reduced whole-bone⁽⁸⁾ and osteoblast-specific Wnt-signaling subsequent to SCI.⁽⁹⁾ As such, pharmacologic sclerostin inhibition (via sclerostin antibody [Scl-Ab]), initiated at or near

the time of injury, may represent a means of preventing bone loss subsequent to SCI,⁽⁷⁾ a possibility that has not been previously examined. Scl-Ab produces bone anabolic effects in other rodent bone loss models, including hindlimb immobilization,⁽¹³⁾ and romosozumab (a clinical sclerostin antibody) has shown promise in the treatment of postmenopausal osteoporosis.⁽¹⁴⁾ However, the nontraditional uncoupling of bone turnover after SCI results in far more severe bone loss than other forms of disuse^(15,16) or sex-hormone deficiency,⁽¹⁷⁾ which indicates the necessity to directly examine Scl-Ab efficacy after SCI.

Testosterone (T) deficiency (ie, hypogonadism) may also exacerbate SCI-induced bone loss⁽¹⁸⁾ because androgens modulate osteoblast differentiation⁽¹⁹⁾ and influence cancellous bone maintenance in males.⁽²⁰⁾ After SCI, 40% to 80% of men exhibit hypogonadism, with a higher incidence and more severe T deficiency occurring closer to time of injury.⁽²¹⁾ Supporting these findings in humans, we have recently developed a young (14-week-old, nonskeletally mature) male contusion rodent SCI model that exhibits T deficiency and severe cancellous bone loss 21 days after injury.⁽²²⁾ In this model, T-enanthate (TE) protects against SCI-induced cancellous bone loss in a dose-dependent manner, with low-dose (replacement) TE partially preserving bone and high-dose TE fully preventing bone loss via antiresorptive actions.⁽²²⁾ However, extension of these findings to an older skeletally mature animal model is necessary because the rapid bone turnover rate in younger animals is not representative of the clinical SCI population.

The primary purpose of this study was to determine whether pharmacologic sclerostin inhibition attenuates cancellous bone loss in a skeletally mature male rodent contusion SCI model. A secondary purpose was to directly compare the bone-protective effects of Scl-Ab to that of TE. We hypothesized that Scl-Ab and TE would each preserve cancellous bone, albeit via differing bone anabolic and antiresorptive effects, respectively.

Materials and Methods

Animal care

Barrier-raised and specific pathogen-free male Sprague-Dawley rats aged approximately 5 months were obtained from Charles River Laboratories (Wilmington, MA, USA). Animals were individually housed in a temperature- and light-controlled room on a 12-hour light/dark cycle. Rats were fed rodent chow containing 3.1 kcal/g, distributed as 58% carbohydrate, 24% protein, and 18% fat (2018 Teklad Global 18% Protein Rodent Diet, Harlan Laboratories Inc., Indianapolis, IN, USA) and tap water *ad libitum*. All experimental procedures conformed to the ILAR Guide to the Care and Use of Experimental Animals and were approved by the Institutional Animal Care and Use Committee at the Gainesville VA Medical Center.

Experimental design

Rats ($n = 11-19$ /group) were blocked by initial weight and randomized into the following groups: (A) Sham surgery (T8 laminectomy) + vehicle (SHAM); (B) T8 laminectomy + moderate-severe (250 kilodyne) contusion SCI + vehicle (SCI); (C) SCI + TE; or (D) SCI + Scl-Ab. SCI + TE animals received TE (7.0 mg/wk for 3 weeks, im) under brief isoflurane

anesthesia, whereas all other groups received vehicle (sesame oil) under the same anesthesia. In this manner, anesthesia exposure was identical between all groups. SCI + Scl-Ab animals received Scl-Ab (25 mg/kg twice weekly for 3 weeks, sc), whereas all other groups received sc saline (vehicle). No anesthesia was required for Scl-Ab/saline administration because agents were administered sc. Animals were assessed for open-field locomotion by two blinded observers using the Basso-Beattie-Bresnahan (BBB) locomotor rating scale⁽²³⁾ at weekly intervals. Declomycin and calcein (all chemicals obtained from Sigma-Aldrich, St. Louis, MO, USA, unless noted) were administered (15 mg/kg, sc) 10 and 3 days before death, respectively, to fluorochrome label actively forming bone surfaces. Animals were euthanized 21 days after surgery via an overdose of pentobarbital (120 mg/kg, ip), blood was collected via cardiac puncture, and left and right femurs and tibiae were excised and weighed. A section of the spinal cord (including the lesion site) was also excised and fixed in 10% formalin for histological analysis to confirm the consistency of injury severity among groups. Blood samples were centrifuged at 3000g, and serum aliquots were separated and stored at -80 °C until analysis. Femurs were wrapped in saline-soaked gauze to prevent dehydration and stored at -20 °C until microcomputed tomography (μ CT) analysis and assessment of bone mechanical properties. Tibiae were fixed in formalin for 48 hours and then stored at 4 °C in 70% ethanol before histomorphometric and μ CT analysis.

Surgery and postoperative care

Animals were kept on a circulating water heated pad to maintain body temperature and remained under isoflurane anesthesia during all surgical procedures. The spinal cord was exposed by laminectomy under sterile conditions, and a 250-kilodyne force was applied to the thoracic (T) 8 segment of the spinal cord using the Infinite Horizons (IH) Impactor (Precision Systems and Instrumentation, Lexington, KY, USA), which induced a moderate-severe mid-thoracic contusion SCI. Confirmation of T8 laminectomy/injury was verified at time of surgery using anatomical landmarks and during spinal column dissection after euthanization.

Animals received buprenorphine (0.05 mg/kg, sc) and ketoprofen (5.0 mg/kg, sc) to reduce pain and inflammation for 48 hours after SCI, and ampicillin was administered for 5 days after surgery. Postoperative animal care included daily examination for signs of distress, weight loss, dehydration, fecal clearance, bladder dysfunction, and skin lesions. Bladders were expressed manually (2 to 3 times daily) until spontaneous voiding returned. Ringer's solution was provided sc to promote rehydration. A nutritional supplement (Jell-O cube with added protein and fat) and apples were provided to expedite recovery and assist in body-weight maintenance.

Animal model and study duration rationales

We have previously reported that moderate-severe contusion SCI produces extensive cancellous bone deficits in young male rats within 21 days of injury⁽²²⁾ and that the majority of cancellous bone loss occurs within the first 7 days of contusion SCI;⁽¹⁶⁾ for this reason, we initiated pharmacologic therapy immediately after surgery. We evaluated a skeletally mature male contusion SCI model for this experiment because the vast majority of clinical SCIs occur in adult males via a blow to the spinal cord followed by a period of compression.

Drug selection rationale

A sclerostin-neutralizing monoclonal antibody (Scl-AbIII, Amgen Inc., Thousand Oaks, CA, USA) was chosen because this agent produces bone anabolic effects in other rodent bone loss models of disuse⁽¹³⁾ and sex-steroid deficiency⁽²⁴⁾ in a similar time frame and at an identical dose to that provided in this study (25 mg/kg twice weekly for 3 weeks, sc). Direct evaluation of this agent after SCI has not been previously reported and is necessary because bone loss after SCI results from a nontraditional uncoupling of bone resorption/formation processes and is more severe than other rodent disuse^(15,16) and sex steroid-deficiency models.⁽¹⁷⁾ Testosterone-enanthate (Savient Pharmaceutical, East Brunswick, NJ, USA) was chosen because this agent produces antiresorptive effects and completely prevents cancellous bone loss in skeletally mature rats after orchietomy⁽²⁰⁾ and in younger (nonskeletally mature) rats after SCI⁽²²⁾ at the dose provided (7.0 mg/wk, im), whereas lower doses only partially prevent bone loss after SCI.⁽²²⁾ In addition, the TE dose and route of administration are similar to that of a clinical trial we recently conducted demonstrating the clinical relevance of this treatment dose,⁽²⁵⁾ and previous meta-analysis data indicate that standard clinical intramuscular T doses improve BMD in ambulatory hypogonadal men, whereas lower (replacement) doses produce no skeletal effect.⁽²⁶⁾ In this manner, our study design allowed direct comparison of a novel osteoanabolic agent (Scl-Ab) versus an established antiresorptive agent (TE) that each address potential factors exacerbating SCI-induced bone loss in a model that mimics the age, sex, and injury characteristics of the largest proportion of the clinical SCI population.

Bone histomorphometry

Cancellous bone parameters were evaluated in the proximal tibial metaphysis using standard histomorphometric techniques, as described previously,⁽²⁷⁾ and follow the recommendations of the Histomorphometry Nomenclature Committee of the American Society of Bone and Mineral Research.⁽²⁸⁾ In brief, tibias were cut cross-sectionally, placed in 10% phosphate-buffered formalin for 48 hr, dehydrated in ethanol, and embedded undecalcified in methyl methacrylate. The proximal tibias were sectioned longitudinally at 4- and 8- μ m thicknesses with a Leica/Jung 2065 microtome. The 4- μ m bone sections were stained with the von Kossa method and counterstained with tetrachrome (Polysciences Inc., Warrington, PA, USA), and the 8- μ m sections remained unstained to measure fluorochrome-based indices of bone formation. The region of interest (ROI) began 1 mm distal to the growth plate and excluded the primary spongiosa and cancellous bone within 0.25 mm of the endocortical surfaces. Cancellous bone structural variables were measured with the Osteomeasure System (Osteometrics, Decatur, GA, USA). Osteoblast (Ob.S/BS) and osteoclast (Oc.S/BS) surfaces were measured as percentages of total cancellous perimeter. Fluorochrome-based indices of cancellous bone formation were measured under ultraviolet illumination. Mineralizing surface (MS/BS), an index of active bone formation, was calculated as the percentage of cancellous bone surface with a double fluorochrome label. Mineral apposition rate (MAR), an index of osteoblast activity, was calculated by dividing the interlabel distance by the time interval between administration of fluorochrome labels. Bone formation rate (BFR/BS) was calculated by multiplying MS/BS by MAR.

μCT analysis of bone morphology

Three-dimensional (3D) bone morphology of the distal femoral and proximal tibial metaphyses was evaluated by high-resolution μCT using a Bruker Skyscan 1172 (Kontich, Belgium) in accordance with previously published methods^(16,20,22) and the recommendations of the American Society of Bone and Mineral Research.⁽²⁹⁾ Images were acquired from the left distal femoral metaphysis and diaphysis using the following parameters: 80 kVP/120μA, 0.5 mm aluminum filter, 1 k camera resolution, 19.9 mm voxel size, 0.5° rotation step, and 180° tomographic rotation and from the proximal tibial metaphysis using the same parameters with the exception of a 2 k camera resolution, 9.8 mm voxel size, 0.7° rotation step. The femoral metaphysis region of interest (ROI) began 1.5 mm proximal to the growth plate and extended 4 mm proximally. The femoral diaphysis ROI encompassed 2 mm at the femoral midshaft. The tibial metaphysis ROI began 1.5 mm distal to the growth plate and extended 2.5 mm distally. Cross-sectional images were reconstructed with a filtered back-projection algorithm (NRecon, Kontich, Belgium). Two-dimensional and 3D morphometric measurements were calculated with CTan software (Bruker Skyscan) and include cancellous bone volume (BV/TV, %), trabecular thickness (Tb.Th, mm), trabecular separation (Tb.Sp, mm), trabecular number (Tb.N, 1/mm), trabecular bone pattern factor (Tb.Pf), and structural model index (SMI). Cortical bone was analyzed at the femoral diaphysis for total cross-sectional area (Tt.Ar, mm²), cortical bone area (Ct.Ar, mm²), medullary area (Ma.Ar, mm²), cortical area fraction (Ct.Ar/Tt.Ar, %), and cortical thickness (Ct.Th, mm).

Bone mechanical evaluation

Subsequent to μCT, the femoral diaphysis underwent a 3-point bending test using a material testing system (Bose ElectroForce 3220, Eden Prairie, MN, USA). The femurs were thawed to room temperature and remained wrapped in saline-soaked gauze except during testing. Femurs were tested at a constant displacement of 0.05 mm/s until failure. The applied force was measured with a 225 N load cell. Test data were sampled at 2500 Hz and analyzed for peak load (N), displacement at failure (mm), stiffness (N/mm), and energy to failure (N × mm).

Spinal cord histology

After fixation and dehydration, the spinal cord was embedded in paraffin and sectioned at 10 μm thickness with a microtome. Hematoxylin and eosin (H&E)-stained sections were evaluated using a Zeiss Axio Imager Z2 light microscope (Carl Zeiss, Göttingen, Germany) at ×2.5 magnification to qualitatively assess injury severity among groups.

Serum measurements

Serum measurements were performed in duplicate on a single plate. Testosterone was determined by EIA with a sensitivity of 0.02 ng/mL and an intra-assay coefficient of variation (CV) <9% (ALPCO Diagnostics, Salem, NH, USA). Sclerostin was determined by ELISA with a sensitivity of 1.63 pg/mL and an intra-assay CV <7.2% (R&D Systems, Minneapolis, MN, USA). Total procollagen type 1 N-terminal propeptide (P1NP) was determined by EIA with a sensitivity of 0.7 ng/mL and an intra-assay CV <7.4%;

osteocalcin was determined by EIA with a sensitivity of 50 ng/mL and an intra-assay CV <5.0%; and C-telopeptide was determined by EIA with a sensitivity of 2.0 ng/mL and an intra-assay CV <9.2% (IDS, Fountain Hills, AZ, USA).

Statistical analysis

Results are reported as mean \pm SEM, with the threshold for significance defined as $p < 0.05$. Mixed-model repeated measures ANOVAs were used to analyze variables that were assessed at multiple time points. One-way ANOVAs and Tukey's post hoc tests (when appropriate) were used to analyze normally distributed data that were assessed at one time point. The nonparametric Kruskal-Wallis and Mann-Whitney U tests were used when data were not normally distributed. Pearson correlation coefficients were used to assess associations between bone mechanical characteristics and cortical bone morphometry at the femoral diaphysis. Data were analyzed with the SPSS version 18.0.0 statistical software package (IBM, Chicago, IL, USA).

Results

Injury severity and locomotor function

The injury force and velocity were 264 ± 7 kilodyne and 122 ± 1 mm/s (SCI), 256 ± 2 kilodyne and 120 ± 1 mm/s (SCI + TE), and 258 ± 2 kilodyne and 121 ± 1 mm/s (SCI + Scl-Ab), respectively, with no differences among groups. Light microscopic analysis of the spinal cord indicated that the injuries appeared symmetrical with loss of white and gray matter on both left and right sides (Supplemental Fig. S1). A thin layer of white matter was spared mostly in the ventral half of the cord. Under higher magnification, the spared white matter revealed some preservation of myelin, axons, and collagen morphology, with significant axonal loss. Moreover, single to multiple cavities were detected in the injured epicenters, which were often filled with dead tissue debris. Overall, histological assessment of the spinal cord verified that a moderate-severe injury intensity was consistently present at the injury epicenter in animals receiving SCI.

Immediately post-injury, the SCI, SCI + TE, and SCI + Scl-Ab groups exhibited a complete loss of hindlimb locomotor function, characteristic of moderate-severe SCI. BBB scores remained significantly lower than SHAM at each time point after injury (Supplemental Fig. S2; $p = 0.01$) and did not differ among injury groups. A similar (expected) degree of locomotor improvement occurred from days 7 to 21 post-injury, with locomotor function remaining below the threshold for weight-supported stepping (ie, BBB = 9) in all injury groups.

Body mass and bone mass/length

No differences in body mass were present among groups at baseline (Supplemental Table S1). SCI produced an expected reduction in body mass, which neither TE nor Scl-Ab prevented. No differences in femur and tibia length/mass were present among groups.

Cancellous bone histomorphometry

Proximal tibial BV/TV was 65% lower in SCI compared with SHAM (Table 1, Fig. 1A–D; $p < 0.001$), characterized by a 57% lower Tb.N ($p < 0.001$), 23% lower Tb.Th ($p < 0.05$), and nearly threefold higher Tb.Sp ($p < 0.01$). In contrast, BV/TV was >twofold higher in SCI + Scl-Ab and SCI + TE animals versus SCI ($p < 0.01$ SCI + Scl-Ab and $p < 0.05$ SCI + TE) and not different from SHAM. Scl-Ab and TE treatments each prevented the SCI-induced reductions in Tb.N ($p < 0.01$), Tb.Th ($p < 0.01$ SCI + Scl-Ab and $p = 0.081$, trend SCI + TE), and Tb.Sp ($p < 0.01$), ultimately maintaining values at SHAM levels.

Oc.S/BS was not different among SHAM, SCI, and SCI + Scl-Ab animals (Table 1), whereas Oc.S/BS in SCI + TE animals was 69% lower than SCI ($p < 0.01$) and 63% lower than SCI + Scl-Ab ($p < 0.05$) in SCI + TE animals. Ob.S/BS was similar in SHAM, SCI, and SCI + TE animals (Table 1) but was roughly fourfold higher in SCI + Scl-Ab animals compared with all other groups ($p < 0.01$).

No significant differences in MS/BS, MAR, or BFR/BS were present among SHAM, SCI, and SCI + TE animals (Table 1). In contrast, SCI + Scl-Ab exhibited a two- to fourfold higher MS/BS ($p < 0.01$) and a two- to fivefold higher BFR/BS ($p < 0.01$) versus all other groups, and a trend for higher mineral apposition rate (MAR) compared with SCI ($p = 0.07$).

μ CT analysis of bone microarchitecture

Similar to histomorphometry, 3D μ CT assessed BV/TV at the proximal tibia and distal femur were 46% to 48% lower in SCI animals versus SHAM (Table 2, Fig. 1E–L; $p < 0.01$ tibia and $p = 0.078$, trend femur) and was characterized by reduced Tb.N d and Tb.Th ($p < 0.05$ tibia and not statistically significant for femur). TE and Scl-Ab fully prevented cancellous BV/TV loss at the distal femur, with values being 72% to 74% higher than SCI ($p < 0.05$) and not different than SHAM, and TE partially prevented tibial BV/TV loss, with values being 64% higher than SCI ($p = 0.063$, trend). BV/TV was primarily preserved via increased Tb.Th in SCI + Scl-Ab animals, with tibial values being 11% to 20% higher than all other groups ($p < 0.001$) and femoral values being 12% higher than SHAM ($p < 0.05$) and 18% higher than SCI ($p < 0.01$). In contrast, BV/TV was primarily preserved in SCI + TE animals via maintenance of Tb.N, with tibial/femoral values being 62% to 71% higher than SCI ($p < 0.05$) and not different than SHAM.

Several cancellous microarchitectural differences were also present among groups (Table 2). In particular, SCI animals exhibited an elevated Tb.Pf ($p < 0.01$ tibia and $p = 0.052$, trend femur) and SMI ($p < 0.05$ tibia and $p < 0.01$ femur) versus SHAM. In contrast, Tb.Pf was lower in SCI + Scl-Ab and SCI + TE compared with SCI alone ($p < 0.05$ tibia in both groups and $p < 0.01$ femur in SCI + Scl-Ab) and not different from SHAM. SMI was also lower in SCI + TE animals compared with SCI ($p < 0.05$ tibia and femur) and not different from SHAM. No femoral diaphysis cortical morphometric differences were present among groups (Supplemental Table S2).

Bone mechanical strength

Peak load was 22% lower in SCI versus SHAM ($p < 0.05$) (Fig. 2). Scl-Ab fully prevented the reduction in peak load, with values being 29% higher in SCI + Scl-Ab relative to SCI ($p < 0.05$) and not different from SHAM, whereas SCI + TE partially prevented the reduction in peak load, with values being not different from SHAM or SCI. No other differences in femoral diaphysis bone mechanical characteristics were observed among groups (Supplemental Table S3). Positive associations were observed between femoral diaphysis peak load and Ct.Th ($r = 0.480$, $p = 0.01$), Ct.Ar ($r = 0.473$, $p = 0.01$), and Ct.Ar/Tt.Ar ($r = 0.349$, $p < 0.05$) at the femoral diaphysis, with no other significant correlations present.

Serum testosterone and bone turnover markers

Serum T was 3.7 ± 1.0 ng/mL (SHAM), 1.7 ± 0.4 ng/mL (SCI), 6.3 ± 0.4 ng/mL (SCI + TE), and 2.4 ± 0.6 ng/mL (SCI + Scl-Ab), with SCI concentrations being 54% lower than SHAM ($p < 0.05$). In contrast, peak circulating T was 70% higher in SCI + TE versus SHAM ($p < 0.05$) and two- to threefold higher than SCI ($p = 0.001$) and SCI + Scl-Ab ($p = 0.01$) animals. Serum sclerostin was 427 ± 30 pg/mL (SHAM), 416 ± 32 pg/mL (SCI), and 342 ± 12 pg/mL (SCI + TE), with no differences between groups. Circulating sclerostin was not measured in SCI + Scl-Ab because of cross-reactivity between the administered Scl-Ab and the assay. Serum CTX-1 was 28 ± 2 ng/mL (SHAM), 42 ± 4 ng/mL (SCI), 43 ± 4 ng/mL (SCI + TE), and 42 ± 2 ng/mL (SCI + Scl-Ab), with all SCI groups being 50% higher than SHAM ($p < 0.05$). Serum P1NP was 58 ± 11 ng/mL (SHAM), 31 ± 2 ng/mL (SCI), 37 ± 3 ng/mL (SCI + TE), and 63 ± 7 ng/mL (SCI + Scl-Ab), with SCI being 47% lower than SHAM ($p < 0.05$) and SCI + Scl-Ab being 100% higher than SCI ($p < 0.001$) and 70% higher than SCI + TE ($p < 0.01$). Serum osteocalcin was 511 ± 22 ng/mL (SHAM), 485 ± 38 ng/mL (SCI), 261 ± 21 ng/mL (SCI + TE), and 543 ± 81 ng/mL (SCI + Scl-Ab), with SCI + TE being 50% lower than all other groups ($p < 0.05$).

Discussion

Functionally complete SCI produces rapid bone loss that results, in part, from elevated sclerostin and reduced Wnt-signaling subsequent to disuse.⁽⁷⁾ To our knowledge, our results provide the first direct evidence indicating that pharmacologic sclerostin inhibition prevents cancellous bone loss subsequent to SCI. Specifically, we observed that moderate-severe contusion SCI produced robust (sublesional) cancellous bone deficits at the proximal tibia and distal femur in skeletally mature male rats within 21 days of injury. These deleterious skeletal adaptations were characterized by reduced Tb.N and Tb.Th and increased Tb.Sp, resulting from elevated bone resorption and a relatively unchanged bone formation consequent to injury. In contrast, sclerostin inhibition produced bone anabolic effects that completely prevented the SCI-induced cancellous bone deficits. In addition, our results confirm previous reports indicating that TE completely prevented hindlimb cancellous bone loss subsequent to SCI, primarily via antiresorptive effects,⁽²²⁾ and extend these results to a skeletally mature animal model. As such, our data indicate that Scl-Ab and TE are promising treatments for preventing cancellous bone loss subsequent to SCI, albeit via differing mechanisms.

Lower-extremity bone loss and high fracture risk are well-known metabolic consequences of functionally complete SCI.⁽¹⁾ The rapid bone loss that occurs in humans subsequent to SCI results from elevated bone resorption and normal or slightly reduced bone formation that produce an uncoupled bone turnover.⁽¹⁾ Likewise, the cancellous bone loss observed in our rodent SCI model resulted from a combination of elevated bone resorption, as indicated by increased CTX-1, and a relatively normal or a slightly reduced bone formation rate, as indicated by reduced serum P1NP and slightly reduced histomorphometric indices of bone formation. These changes confirm what has been reported clinically⁽¹⁾ and experimentally in our laboratory⁽²²⁾ and by others.⁽¹⁷⁾ SCI also reduced trabecular connectivity (ie, increased Tb.Pf) and platelike trabecular geometry (ie, increased SMI), indicating deleterious microarchitectural alterations persist in the remaining trabecular network after SCI. These changes suggest compromised structural integrity and reduced mechanical strength in the cancellous network. Interestingly, SCI also produced a reduction in whole-bone strength at the femoral diaphysis, a site comprised almost entirely of cortical bone, despite the fact that no cortical morphometric differences were observed at this skeletal site via μ CT. The loss in mechanical strength may have resulted from very slight (nonsignificant) reductions in cortical thickness and cortical area because these morphometric variables were positively associated with peak load at the femoral diaphysis. Alternatively, deleterious microstructural alterations (eg, increased cortical porosity), which have been reported after disuse,⁽³⁰⁾ may underlie SCI-induced reductions in cortical bone strength. Unfortunately, we could not evaluate this possibility because of our a priori selection of μ CT scanning parameters and the destructive nature of the bone mechanical evaluation. As such, this remains an interesting area of future study.

The primary cause of SCI-induced bone loss is disuse subsequent to the neural insult. In this regard, mechanical loading is known to influence SOST expression, the gene that encodes for the protein sclerostin.⁽³¹⁾ Sclerostin is an endogenous osteocyte-derived negative regulator of the Wnt-signaling pathway that promotes osteoblast development.⁽⁷⁾ For example, hindlimb unloading increases sclerostin mRNA⁽³²⁾ and protein expression in osteocytes, whereas electrically stimulated muscle contractions ablate this effect.⁽³³⁾ Elevated sclerostin induces bone loss by binding the Wnt co-receptor lipoprotein receptor-related protein (LRP) 5–6, which prevents Wnt signaling-induced bone accretion.⁽⁷⁾ As evidence, overexpression of sclerostin gene alleles results in high sclerostin and severe osteopenia.⁽³⁴⁾ Alternatively, targeted deletion of the sclerostin gene increases bone formation, resulting in an extremely high bone mass phenotype and increased bone strength.⁽³⁵⁾ Sclerostin also appears to play a role in bone loss subsequent to SCI, especially given that 1) elevated circulating sclerostin persists for several years in individuals with functionally complete SCI⁽¹²⁾ and 2) rodents exhibit reduced whole-bone⁽⁸⁾ and osteoblast-specific Wnt signaling and LRP5 expressions subsequent to SCI.^(9,10)

Herein, we present the first-ever data indicating that pharmacologic sclerostin inhibition prevents cancellous bone loss subsequent to SCI. This effect occurred through direct bone anabolic actions, as evidenced by elevated osteoblast surface and increased bone formation rates in SCI + Scl-Ab animals. Interestingly, serum osteocalcin (a circulating marker of bone formation) was not elevated by Scl-Ab treatment, an effect that remains difficult to explain given the clear histomorphometric evidence supporting elevated bone

formation induced by Scl-Ab. In contrast, P1NP (a circulating marker of type I collagen deposition) was reduced by SCI, an effect that was completely prevented by Scl-Ab. In this regard, P1NP appears to be a more robust circulating bone formation marker than osteocalcin after SCI, given the similarities between our P1NP and histomorphometric findings. Alternatively, it remains possible that we missed the peak circulating osteocalcin value because elevations in circulating osteocalcin are somewhat transient after Scl-Ab administration, occurring primarily at the initiation of treatment and declining thereafter, in both preclinical models⁽²⁴⁾ and clinically.⁽¹⁴⁾ Regardless, our data support a growing number of preclinical studies demonstrating the efficacy of Scl-Ab treatment in preventing bone loss in models of disuse⁽¹³⁾ and sex-steroid deficiency.⁽²⁴⁾ Additionally, we observed that Scl-Ab improved trabecular connectivity, evidenced by a lower Tb.Pf in the hindlimbs compared with SCI alone, suggesting structurally improved mechanical strength of the trabecular network. Further, Scl-Ab completely prevented the loss of whole-bone mechanical strength at the femoral diaphysis resulting from SCI, which suggests beneficial cortical adaptations occurred in SCI + Scl-Ab animals; however, we did not detect cortical morphometric differences among groups, likely because of the abbreviated (21-day) duration of this study. Clearly, longer-term studies evaluating the effects of Scl-Ab on cortical bone morphometry and skeletal regeneration after SCI are warranted.

Several other secondary consequences of SCI may also exacerbate skeletal deterioration after injury, including hypogonadism,⁽¹⁸⁾ which is at least partially influenced by pituitary dysfunction, as evidenced by elevated luteinizing hormone and follicle-stimulating hormone compared with able-bodied individuals.⁽³⁶⁾ In particular, men with SCI exhibit more severe hypogonadism closer to time of injury,⁽²¹⁾ corresponding with the time frame of the most rapid cancellous bone loss after SCI. We have previously reported that young male rodents also exhibit low circulating T for at least 21 days after contusion SCI and that low-dose (replacement) TE partially preserves bone subsequent to SCI,⁽²²⁾ demonstrating that T deficiency influences SCI-induced bone loss. Interestingly, in the aforementioned study, high-dose TE completely prevented SCI-induced bone loss, suggesting that pharmacologic T doses are necessary for full bone preservation.⁽²²⁾ Similarly, in ambulatory hypogonadal men, higher-than-replacement (intramuscular) T improves BMD, whereas replacement doses produce no effect on BMD.⁽²⁶⁾ Our current study expands on the previously mentioned findings by demonstrating for the first time that TE completely prevents cancellous bone deficits in skeletally mature rodents, the importance of which extends to the vast majority of men who experience SCI in adulthood. However, TE did not completely preserve cortical bone (femoral diaphysis) strength, possibly suggesting that TE exerts divergent effects in cancellous and cortical bone. Interestingly, a similar degree of cancellous BV/TV and microarchitectural maintenance was present in SCI + TE and SCI + Scl-Ab animals, albeit via differing antiresorptive and bone anabolic effects, respectively. In this regard, the effects of TE on bone are primarily antiresorptive, as evidenced by the reduced osteoclast surface in SCI + TE animals, which corroborates previous findings from our laboratory.⁽²²⁾ However, we were unable to detect reductions in circulating CTX-1 in our current or previous studies,⁽²²⁾ perhaps because the vast majority of cancellous bone loss appears to occur relatively quickly after SCI,⁽¹⁶⁾ whereas blood was acquired at a later time point.

Despite the rapid bone loss and high fracture incidence that occur subsequent to SCI, no clinical guidelines currently address osteoporosis treatment in this population.⁽⁷⁾ Bisphosphonate administration is the primary pharmacologic therapy administered to individuals with SCI-induced osteoporosis.⁽³⁷⁾ However, long-term bisphosphonate therapy only slows bone loss after SCI but does not completely eliminate bone demineralization nor regenerate bone at sublesional skeletal sites,⁽³⁸⁾ necessitating alternative treatments for the SCI population. In this regard, our current and previous⁽²²⁾ results provide rationale for future clinical trials assessing the effectiveness of TE as a means of preventing bone loss subsequent to SCI. Certainly, the preclinical results presented herein also provide rationale for future clinical trials assessing whether sclerostin-neutralizing antibodies prevent bone loss in clinical SCI populations, especially in light of the recent clinical evidence demonstrating that romosozumab has shown rapid and robust increases in BMD in postmenopausal women.⁽¹⁴⁾

In conclusion, we present the first evidence demonstrating that pharmacologic sclerostin inhibition prevents SCI-induced cancellous bone deficits and preserves whole-bone strength in skeletally mature male rats, primarily via bone anabolic effects. Interestingly, TE also prevented cancellous bone deficits and the deleterious microarchitectural alterations in the cancellous network that occur subsequent to SCI, albeit via antiresorptive effects. The observation that Scl-Ab and TE both maintain cancellous bone through apparently differing mechanisms raises the unique possibility that Scl-Ab and TE may produce complementary skeletal effects when administered simultaneously, especially considering that bone loss subsequent to SCI results from a nontraditional uncoupling of bone resorption/formation processes, although this remains to be evaluated in future studies.

Supplementary Material

Refer to Web version on PubMed Central for supplementary material.

Acknowledgments

This work was supported by resources provided by the North Florida/South Georgia Veterans Health System and by work supported by the Office of Research and Development, Rehabilitation Research and Development (RR&D) Service, Department of Veterans Affairs (VA RR&D SPiRE 1I21RX001371-01 to JFY, CDA-2 B7733-W to JFY, and VA RR&D Merit Award AR 6884R to SEB). FY is supported by a Paralyzed Veterans of America postdoctoral fellowship. Sclerostin antibody was generously provided by Amgen, Inc., through a Department of Veterans Affairs Cooperative Research and Development Agreement (CRADA). “The contents do not represent the views of the US Department of Veterans Affairs or the United States Government.”

References

1. Zehnder Y, Luthi M, Michel D, et al. Long-term changes in bone metabolism, bone mineral density, quantitative ultrasound parameters, and fracture incidence after spinal cord injury: a cross-sectional observational study in 100 paraplegic men. *Osteoporos Int.* 2004;15:180–9. [PubMed: 14722626]
2. Dauty M, Perrouin Verbe, Maugars B, Dubois Y, Mathe C. Supralesional and sublesional bone mineral density in spinal cord-injured patients. *Bone.* 2000;27:305–9. [PubMed: 10913927]
3. Eser P, Frotzler A, Zehnder Y, et al. Relationship between the duration of paralysis and bone structure: a pQCT study of spinal cord injured individuals. *Bone.* 2004;34:869–80. [PubMed: 15121019]

4. Frisbie JH. Fractures after myelopathy: the risk quantified. *J Spinal Cord Med.* 1997;20:66–9. [PubMed: 9097259]
5. Szollar SM, Martin EM, Sartoris DJ, Parthemore JG, Deftos LJ. Bone mineral density and indexes of bone metabolism in spinal cord injury. *Am J Phys Med Rehabil.* 1998;77:28–35. [PubMed: 9482376]
6. Morse LR, Battaglini RA, Stolzmann KL, et al. Osteoporotic fractures and hospitalization risk in chronic spinal cord injury. *Osteoporos Int.* 2009;20:385–92. [PubMed: 18581033]
7. Battaglini RA, Lazzari AA, Garshick E, Morse LR. Spinal cord injury-induced osteoporosis: pathogenesis and emerging therapies. *Curr Osteoporos Rep.* 2012;10:278–85. [PubMed: 22983921]
8. Yan J, Li B, Chen JW, Jiang SD, Jiang LS. Spinal cord injury causes bone loss through peroxisome proliferator-activated receptor-gamma and Wnt signalling. *J Cell Mol Med.* 2012;16: 2968–77. [PubMed: 22947224]
9. Jiang SD, Yan J, Jiang LS, Dai LY. Down-regulation of the Wnt, estrogen receptor, insulin-like growth factor-I, and bone morphogenetic protein pathways in osteoblasts from rats with chronic spinal cord injury. *Joint Bone Spine.* 2011;78:488–92. [PubMed: 21273111]
10. Sun L, Pan J, Peng Y, et al. Anabolic steroids reduce spinal cord injury-related bone loss in rats associated with increased Wnt signaling. *J Spinal Cord Med.* 2013;36:616–22. [PubMed: 24090150]
11. Morse LR, Sudhakar S, Danilack V, et al. Association between sclerostin and bone density in chronic spinal cord injury. *J Bone Miner Res.* 2012;27:352–9. [PubMed: 22006831]
12. Battaglini RA, Sudhakar S, Lazzari AA, Garshick E, Zafonte R, Morse LR. Circulating sclerostin is elevated in short-term and reduced in long-term SCI. *Bone.* 2012;51:600–5. [PubMed: 22575440]
13. Tian X, Jee WS, Li X, Paszty C, Ke HZ. Sclerostin antibody increases bone mass by stimulating bone formation and inhibiting bone resorption in a hindlimb-immobilization rat model. *Bone.* 2011; 48:197–201. [PubMed: 20850580]
14. McClung MR, Grauer A, Boonen S, et al. Romosozumab in postmenopausal women with low bone mineral density. *N Engl J Med.* 2014;370:412–20. [PubMed: 24382002]
15. Liu D, Zhao CQ, Li H, Jiang SD, Jiang LS, Dai LY. Effects of spinal cord injury and hindlimb immobilization on sublesional and supralesional bones in young growing rats. *Bone.* 2008; 43:119–25. [PubMed: 18482879]
16. Yarrow JF, Ye F, Balazs A, et al. Bone loss in a new rodent model combining spinal cord injury and cast immobilization. *J Musculoskelet Neuronal Interact.* 2014;14:255–66. [PubMed: 25198220]
17. Jiang SD, Shen C, Jiang LS, Dai LY. Differences of bone mass and bone structure in osteopenic rat models caused by spinal cord injury and ovariectomy. *Osteoporos Int.* 2007;18:743–50. [PubMed: 17216554]
18. Jiang SD, Jiang LS, Dai LY. Mechanisms of osteoporosis in spinal cord injury. *Clin Endocrinol (Oxf).* 2006; 65:555–65. [PubMed: 17054455]
19. Liu XH, Kirschenbaum A, Yao S, Levine AC. Androgens promote preosteoblast differentiation via activation of the canonical Wnt signaling pathway. *Ann NY Acad Sci.* 2007;1116:423–31. [PubMed: 17646262]
20. Beck DT, Yarrow JF, Beggs LA, et al. Influence of aromatase inhibition on the bone protective effects of testosterone. *J Bone Miner Res.* 2014;29:2405–13. [PubMed: 24764121]
21. Clark MJ, Schopp LH, Mazurek MO, et al. Testosterone levels among men with spinal cord injury: relationship between time since injury and laboratory values. *Am J Phys Med Rehabil.* 2008;87:758–67. [PubMed: 18716488]
22. Yarrow JF, Conover CF, Beggs LA, et al. Testosterone dose dependently prevents bone and muscle loss in rodents after spinal cord injury. *J Neurotrauma.* 2014;31:834–45. [PubMed: 24378197]
23. Basso DM, Beattie MS, Bresnahan JC. Graded histological and locomotor outcomes after spinal cord contusion using the NYU weight-drop device versus transection. *Exp Neurol.* 1996;139:244–56. [PubMed: 8654527]
24. Li X, Ominsky MS, Warmington KS, et al. Sclerostin antibody treatment increases bone formation, bone mass, and bone strength in a rat model of postmenopausal osteoporosis. *J Bone Miner Res.* 2009;24:578–88. [PubMed: 19049336]

25. Borst SE, Yarrow JF, Conover CF, et al. Musculoskeletal and prostate effects of combined testosterone and finasteride administration in older hypogonadal men: a randomized, controlled trial. *Am J Physiol Endocrinol Metab.* 2014;306:E433–42. [PubMed: 24326421]
26. Tracz MJ, Sideras K, Bolona ER, et al. Testosterone use in men and its effects on bone health. A systematic review and meta-analysis of randomized placebo-controlled trials. *J Clin Endocrinol Metab.* 2006;91:2011–6. [PubMed: 16720668]
27. Yarrow JF, Conover CF, Purandare AV, et al. Supraphysiological testosterone enanthate administration prevents bone loss and augments bone strength in gonadectomized male and female rats. *Am J Physiol Endocrinol Metab.* 2008;295:E1213–22. [PubMed: 18780767]
28. Dempster DW, Compston JE, Drezner MK, et al. Standardized nomenclature 2012; update of the report of the ASBMR Histomorphometry Nomenclature Committee. *J Bone Miner Res.* 2013;28:2–17. [PubMed: 23197339]
29. Bouxsein ML, Boyd SK, Christiansen BA, Guldberg RE, Jepsen KJ, Muller R. Guidelines for assessment of bone microstructure in rodents using micro-computed tomography. *J Bone Miner Res.* 2010;25:1468–86. [PubMed: 20533309]
30. Kazakia GJ, Tjong W, Nirody JA, et al. The influence of disuse on bone microstructure and mechanics assessed by HR-pQCT. *Bone.* 2014;63:132–40. [PubMed: 24603002]
31. Tu X, Rhee Y, Condon KW, et al. Sost downregulation and local Wnt signaling are required for the osteogenic response to mechanical loading. *Bone.* 2012;50:209–17. [PubMed: 22075208]
32. Robling AG, Niziolek PJ, Baldridge LA, et al. Mechanical stimulation of bone in vivo reduces osteocyte expression of Sost/sclerostin. *J Biol Chem.* 2008;283:5866–75. [PubMed: 18089564]
33. Macias BR, Swift JM, Nilsson MI, Hogan HA, Bouse SD, Bloomfield SA. Simulated resistance training, but not alendronate, increases cortical bone formation and suppresses sclerostin during disuse. *J Appl Physiol* 1985;112:918–25.
34. Winkler DG, Sutherland MK, Geoghegan JC, et al. Osteocyte control of bone formation via sclerostin, a novel BMP antagonist. *EMBO J.* 2003;22:6267–76. [PubMed: 14633986]
35. Li X, Ominsky MS, Niu QT, et al. Targeted deletion of the sclerostin gene in mice results in increased bone formation and bone strength. *J Bone Miner Res.* 2008;23:860–9. [PubMed: 18269310]
36. Gaspar AP, Brandao CM, Lazaretti-Castro M. Bone mass and hormone analysis in spinal cord injury patients: evidences for a gonadal axis disruption. *J Clin Endocrinol Metab.* Epub 2014; Sep15: jc20142165.
37. Morse LR, Giangregorio L, Battaglini RA, et al. VA-based survey of osteoporosis management in spinal cord injury. *PM.R.* 2009;1:240–4. [PubMed: 19627901]
38. Chang KV, Hung CY, Chen WS, Lai MS, Chien KL, Han DS. Effectiveness of bisphosphonate analogues and functional electrical stimulation on attenuating post-injury osteoporosis in spinal cord injury patients—a systematic review and meta-analysis. *PLoS One.* 2013;8:e81124. [PubMed: 24278386]

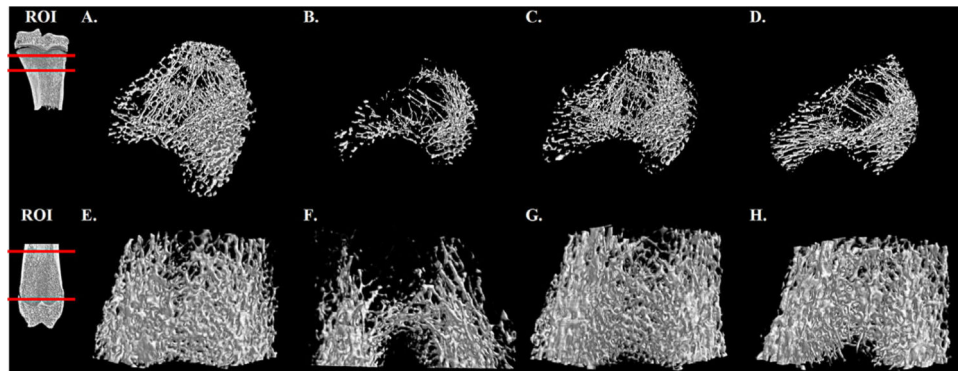


Fig. 1. Representative microcomputed tomography (μ CT) images of cancellous bone at the proximal tibial (*A–D*) and distal femoral metaphysis (*E–H*) regions of interest (ROI) from animals receiving SHAM surgery, moderate-severe contusion spinal cord injury (SCI), SCI + testosterone enanthate (SCI + TE), or SCI + sclerostin antibody (SCI + Scl-Ab). Note reduced trabecular spicules (*B* and *F*) indicative of cancellous osteopenia in SCI rats. Both TE and Scl-Ab prevented cancellous bone loss. Data are presented in Table 2.

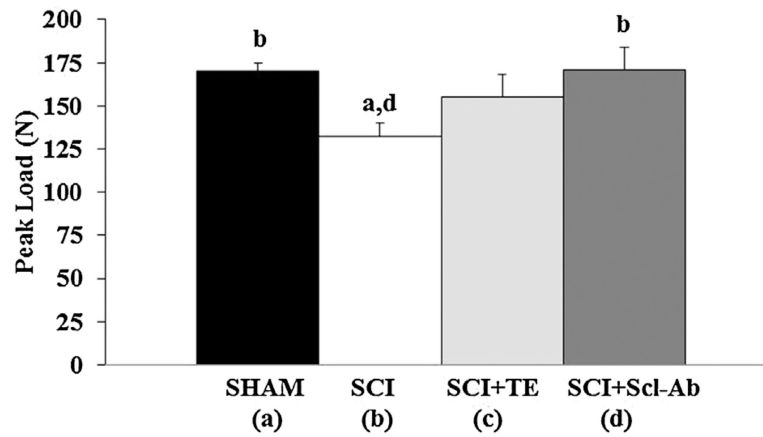


Fig. 2. Peak load at the femoral diaphysis assessed via three-point bending test from animals receiving SHAM surgery, moderate-severe contusion spinal cord injury (SCI), SCI + testosterone enanthate (SCI + TE), or SCI + sclerostin antibody (SCI + Scl-Ab). Data are mean \pm SE from $n = 7-10$ /group. Letters a-d indicate differences from respectively labeled groups at $p < 0.05$.

Table 1. Cancellous Histomorphometric Parameters at the Proximal Tibial Metaphysis From Animals Receiving SHAM Surgery, Moderate-Severe Contusion Spinal Cord Injury (SCI), SCI + Testosterone-Enanthate (SCI + TE), or SCI + Sclerostin Antibody (SCI + Scl-Ab)

	SHAM (a)	SCI (b)	SCI+TE (c)	SCI+Scl-Ab (d)
BV/TV (%)	13.7 ± 1.5 ^{b*}	4.8 ± 0.9 ^{a*,c,d*}	11.7 ± 1.7 ^b	12.3 ± 1.8 ^{b*}
Tb.N (#/mm)	3.0 ± 0.3 ^{b*}	1.3 ± 0.2 ^{a*,c*,d*}	2.7 ± 0.3 ^{b*}	2.5 ± 0.3 ^{b*}
Tb.Th (µm)	45.7 ± 1.8 ^b	35.3 ± 2.2 ^{a,d*}	43.5 ± 2.9	48.2 ± 2.2 ^{b*}
Tb.Sp (µm)	311 ± 34	1158 ± 254 ^{a*,c*,d*}	369 ± 51 ^{b*}	392 ± 43 ^{b*}
Oc.S/BS (%)	4.3 ± 0.7	5.8 ± 0.7 ^{c*}	1.8 ± 0.4 ^{b*,d}	4.9 ± 1.0 ^c
Ob.S/BS (%)	4.1 ± 2.0	4.0 ± 1.3 ^{d*}	4.9 ± 1.3 ^{d*}	17.7 ± 3.4 ^{a*,b*,c*}
MS/BS (%)	10.8 ± 1.6 ^{d*}	7.6 ± 1.4 ^{d*}	14.9 ± 2.7 ^{d*}	29.3 ± 2.5 ^{a*,b*,c*}
MAR (µm/d)	0.9 ± 0.1	0.8 ± 0.1	1.0 ± 0.1	1.2 ± 0.1
BFR/BS (µm ³ /µm ² /d)	10.7 ± 2.6 ^{d*}	6.69 ± 1.8 ^{d*}	15.6 ± 3.9 ^d	37.6 ± 6.0 ^{a*,b*,c}

Data are mean ± SE from n = 9–11/group.

BV/TV = % cancellous bone volume; Tb.Th = trabecular thickness; Tb.N = trabecular number; Tb.Sp = trabecular separation; Oc.S/BS = osteoclast surface; Ob.S/BS = osteoblast surface; MS/BS = mineralizing surface; MAR = mineral apposition rate; BFR/BS = bone formation rate.

^{a-d} Indicate differences from respectively labeled groups at *p* < 0.05 or ***p* < 0.01.

Table 2. μ CT- Derived Cancellous Morphometric Parameters at the Distal Femoral and Proximal Tibial Metaphyses from Animals Receiving SHAM Surgery, Moderate-Severe Contusion Spinal Cord Injury (SCI), SCI+ Testosterone-Enanthate (SCI+TE), or SCI+ Sclerostin Antibody (SCI+Scl-Ab)

	SHAM (a)	SCI (b)	SCI+TE (c)	SCI+Scl-Ab (d)
Distal femoral metaphysis				
BV/TV (%)	14.8 ± 1.8	9.2 ± 1.0 ^{c,d}	16.0 ± 1.8 ^b	15.8 ± 2.6 ^b
Tb.N (#/mm)	1.1 ± 0.1	0.8 ± 0.1 ^c	1.3 ± 0.1 ^b	1.0 ± 0.1
Tb.Th (mm)	0.119 ± 0.003 ^d	0.113 ± 0.002 ^{d*}	0.121 ± 0.004	0.133 ± 0.005 ^{a,b*}
Tb.Sp (mm)	0.69 ± 0.07	0.63 ± 0.04	0.48 ± 0.03	0.58 ± 0.07
Tb.Pf	11.1 ± 0.8	14.2 ± 0.7 ^{d*}	11.2 ± 1.1	9.6 ± 1.1 ^{b*}
SMI	2.28 ± 0.08 ^{b*}	2.63 ± 0.06 ^{a*,c}	2.32 ± 0.09 ^b	2.41 ± 0.11
Proximal tibial metaphysis				
BV/TV (%)	10.5 ± 1.5 ^{b*}	5.7 ± 0.6 ^{a*}	9.4 ± 1.0	8.3 ± 1.3
Tb.N (#/mm)	1.1 ± 0.1 ^b	0.7 ± 0.1 ^{a,c}	1.2 ± 0.1 ^b	0.9 ± 0.1
Tb.Th (mm)	0.081 ± 0.001 ^{b,d*}	0.075 ± 0.001 ^{a,d*}	0.078 ± 0.002 ^{d*}	0.090 ± 0.002 ^{a*,b*,c*}
Tb.Sp (mm)	0.45 ± 0.05	0.54 ± 0.04 ^c	0.38 ± 0.03 ^b	0.48 ± 0.05
Tb.Pf	18.6 ± 1.1 ^{b*}	23.5 ± 0.7 ^{b*,c,d}	19.2 ± 1.1 ^b	18.9 ± 1.3 ^b
SMI	2.49 ± 0.06 ^b	2.72 ± 0.04 ^{a,c}	2.49 ± 0.06 ^b	2.64 ± 0.07

Data are mean ± SE from n = 11–19/group.

μ CT = microcomputed tomography; BV/TV = % cancellous bone volume; Tb.N = trabecular number; Tb.Th = trabecular thickness; Tb.Sp = trabecular separation; Tb.Pf = trabecular pattern factor; SMI = structure model index.

^{a-d} Indicate differences from respectively labeled groups at $p < 0.05$ or $*p < 0.01$.